Groundwater

Source and Quality of Groundwater Surrounding the Qinghai Lake, NE Qinghai–Tibet Plateau

by Dong-sheng Li[1], Bu-li Cui[1,2,3], Ying Wang[1], Ya-Xuan Wang[1], and Bao-Fu Jiang[1]

Abstract

Comprehensive studies on the spatial distribution, water quality, recharge source, and hydrochemical evolution of regional groundwater form the foundation of rational utilization of groundwater resources. In this study, we investigated the water levels, hydrochemistry, and stable isotope composition of groundwater in the vicinity of the Qinghai Lake in China to reveal its recharge sources, hydrochemical evolution, and water quality. The level of groundwater relative to the level of water in the Qinghai Lake ranged from −1.27 to 122.91 m, indicating most of the groundwater to be flowing into the lake. The local evaporation line (LEL) of groundwater was simulated as $\delta^2H = 6.08\ \delta^{18}O$-3.01. The groundwater surrounding the Qinghai Lake was primarily recharged through local precipitation at different altitudes. The hydrochemical type of most of the groundwater samples was Ca-Mg-HCO_3; the hydrochemistry was primarily controlled by carbonate dissolution during runoff. At several locations, the ionic concentrations in groundwater exceeded the current drinking water standards making it unsuitable for drinking. The main source of nitrate in groundwater surrounding the Qinghai Lake was animal feces and sewage, suggesting that groundwater pollution should be mitigated in areas practicing animal husbandry in the Qinghai-Tibet Plateau, regardless of industrial and urbanization rates being relatively low in the region. The scientific planning, engineering, and management of livestock manure and wastewater discharge from animal husbandry practices is a crucial and is urgently required in the Tibetan Plateau.

Introduction

Groundwater is a life-sustaining resource that is utilized as drinking water by 1.5 billion people around the world (Alley et al. 2002). It plays significant roles in agriculture, health of ecosystems, and sustainable development of human societies and economies as well, especially in cold and semiarid regions, where surface water resources are relatively deficient (Qiu 2010; Gleeson et al. 2012, 2016; Van Loon et al. 2016). In recent years, groundwater quality has been compromised by the intensification of human activities as well as by global climate change, and thus, has attracted extensive attention worldwide (Li et al. 2013). Previous studies have reported groundwater levels to have fallen at a phenomenal rate on both regional and global scales (Postel et al. 1996; Oki and Kanae 2006; Rodell et al. 2009; Gleeson et al. 2012). Continuous exploitation of groundwater would lead to a series of severe environmental and ecological problems, such as ground subsidence, aquifer unwatering, salt water intrusion, and ecological degeneration (Edmunds 2009; Liu et al. 2015; Goldin 2016). Therefore, comprehensive studies on the spatial distribution, water quality, recharge sources, and hydrochemical evolution of regional groundwater form the foundation for the rational utilization of groundwater resources. Such studies will inform steps toward scientific management and sustainable development of regional water resources (Chang and Wang 2010; Qiu 2010; Van Loon et al. 2016).

The integrated application of hydrochemistry and isotope characterization is known well as an effective method to revealing the complex hydrological processes, especially in the groundwater cycle (Gibson et al. 2005; Cui and Li 2014; Raghavendra and Deka 2015). For example, Bicalho et al. (2019) used geochemical and isotopic tracers ($\delta^{18}O$, δ^2H, $^{87}Sr/^{86}Sr$, and $\delta^{13}C_{TDIC}$) to constrain origins and chemical evolution of groundwater in a Mediterranean karst system. Younas et al. (2019) evaluated the recharge sources and geochemical characteristics of groundwater in semiarid alluvial aquifers in Pakistan based on isotopic data. Li et al. (2019) investigated the formation mechanism and mixing behavior of the Nanyang thermal spring based on isotopic and hydrochemical techniques. Tweed et al. (2020) investigated the

[1]School of Resources and Environmental Engineering, Ludong University, No.186, Hongqi Mid-Road, Yantai,264025, China

[2]Corresponding author: School of Resources and Environmental Engineering, Ludong University, No. 186 Hongqizhong Street, Yantai, Shandong, 264025, China; +86-535-18953511817; cuibuli@163.com

[3]State Key Laboratory of Loess and Quaternary Geology, Institute of Earth Environment, Chinese Academy of Sciences, No.97, Yanxiang Road, Xi'an,710061, China

Received April 2020, accepted August 2020.

doi: 10.1111/gwat.13042

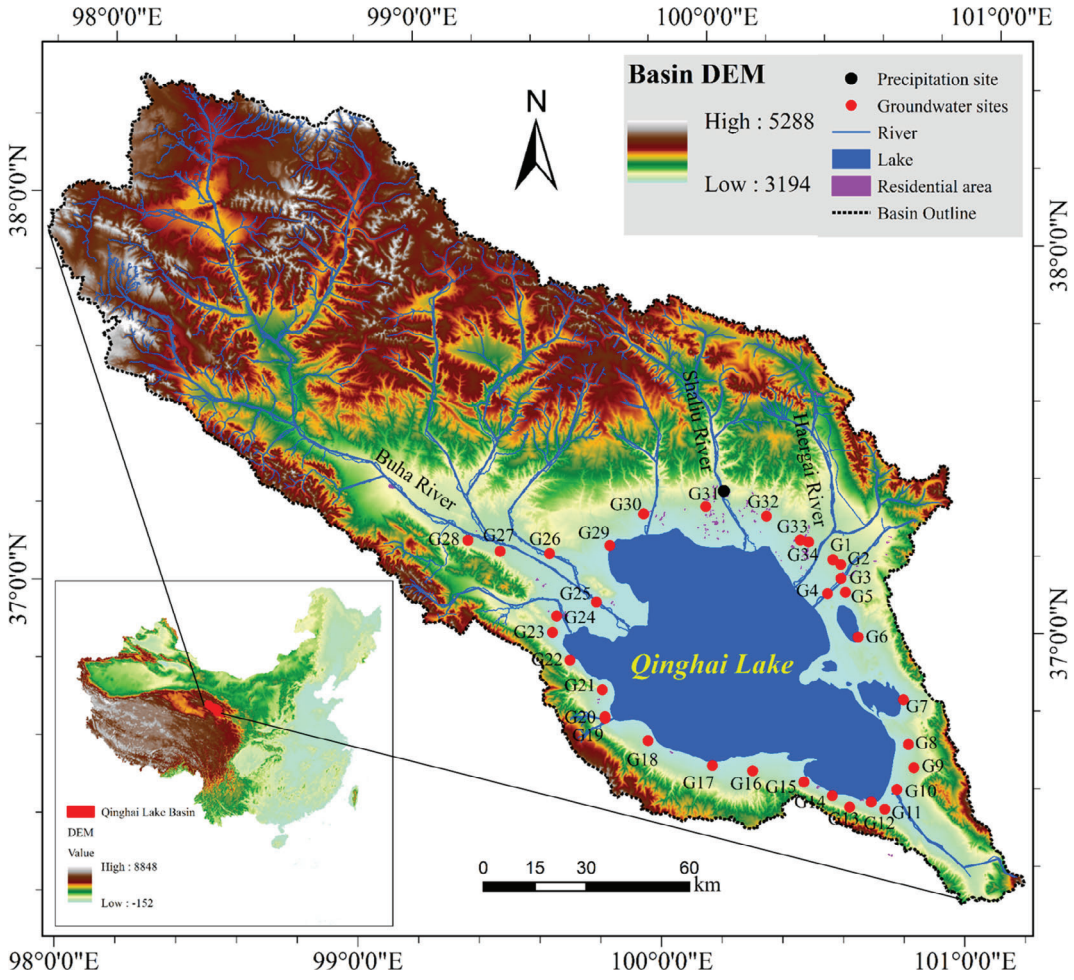

Figure 1. Location of the Qinghai Lake Basin and sampling sites for precipitation and groundwater.

natural and pumping-induced changes in hydrogeological processes in the Cambodian Mekong Delta by using environmental tracers ($\delta^{18}O$, $\delta^{2}H$, ^{3}H, major/trace ions and rare earth elements). Based on the hydrogeochemical and water stable isotope analyses of 23 springs, 10 boreholes, 5 rain-collectors, and 5 leaching-rocks samples at Aconcagua Basin, Taucare et al. (2020) addressed the Western Andean Front hydrogeology. All of these studies demonstrated the applicability and value of isotopes and ions as conservative tracers for hydrologic research, particularly for groundwater systems with complex hydrological processes in arid regions.

The Qinghai Lake, in the north-eastern Tibetan Plateau (NETP), is the largest salt water lake in China with an area of 4264 km^2 (Figure 1). It is an important water body for maintaining ecological security of the NETP (Cui and Li 2015a; Li et al. 2018). Meanwhile, it is a key area for social and economic development in the Qinghai Province because of the extensive ecological tourism and animal husbandry (Li et al. 2018). Furthermore, the Qinghai Lake Basin is an ideal area to study global climate change and uplift processes as well as the water cycle and eco-hydrological processes in the Tibetan Plateau (TP) because of its sensitivity to global climate change and the closed nature of its basin. In recent decades, a series of environmental and ecological problems have arisen due to climate change and unchecked human activities, such as grassland degradation, wetland reduction, and biodiversity decline, that have attracted attention of local governments as well as the international community (Xin 2008; Cui et al. 2016; Li et al. 2018). Previous studies that dealt with the geochemistry and water cycle of the Qinghai Lake Basin focused mainly on paleoclimate and environmental changes, lake evolution and its response to climate change, sources of precipitation, and characteristics of river runoff (Chang et al. 2009; Cui and Li 2015a, 2015b; Tang et al. 2018). However, only a few studies have used stable isotope composition and hydrochemical techniques to investigate the sources and quality of groundwater surrounding the Qinghai Lake (Xiao et al. 2013; Cui and Li 2014).

Therefore, in this study, the objectives were (1) to investigated the characteristics of water level, hydrochemistry, and stable isotope composition of groundwater surrounding the Qinghai Lake, (2) to assess quality of groundwater for drinking purposes by analyzing ion concentrations (total hardness [TH]; total dissolved solids [TDS]; and Na^{+}, Cl^{-}, SO_4^{2-}, and NO_3^{-} content]), and (3) to explore the possible causes of changes of hydrochemistry and isotopes of groundwater. Our results would

contribute to the knowledge regarding hydrological processes of groundwater in the vicinity of salt water lakes in the TP and inform water resource management in the basin.

Study Area

Qinghai Lake lies in the cold and semiarid region of the NETP (Figure 1). It has a closed basin with an area of 29,661 km^2 (36°15′-38°20′N, 97°50′-101°20′E) that lies in a critical transitional zone, where winter westerlies, Southeast Asian monsoon, and the TP monsoon meet (Li et al. 2018). The area and water surface altitude of the Qinghai Lake are 4425 km^2 and 3195.82 m above sea level (a.s.l.), respectively. The salinity and pH of lake water are 15.5 g/L and 9.06, respectively. The ion content in lake water is in the order of $Na^+ > Mg^{2+} > K^+ > Ca^{2+}$ and $Cl^- > SO_4^{2-} > CO_3^{2-} > NO_3^-$ (Sun et al. 1991). The average annual air temperature and precipitation are −0.1 °C and 357 mm, respectively (Cui and Li 2015a). More than 50 streams flow into the lake, most from the west and the north. The largest are the Buha, Shaliu, and Haergai rivers, which account for 75 of surface water inflow. The groundwater aquifers in the basin are primarily alluvial, carbonate, intrusive rock, and clastic rock aquifers, corresponding to the Quaternary deposits, late Paleozoic marine limestone and sandstones, Triassic granite, and Silurian sandstone and schist, respectively (Cui and Li 2014). The average depth of groundwater ranges from 4 to 7 m in the vicinity of the Qinghai Lake, where the groundwater depths are shallowest in sparsely populated areas (Xiao et al. 2012).

Data Source and Methods

Precipitation samples were collected during every precipitation event in the period from January to December, 2018, at the meteorological bureau of Gangcha (3301.5 m a.s.l.), Qinghai Province, China. In total, 104 precipitation samples were collected, including 21 samples of snow or sleet and 83 samples of rain water. Precipitation samples were then filtered using 0.45-μm nylon filters and were stored in 30-mL high-density polyethylene bottles for isotopic analyses.

In September 2018, groundwater samples were collected from 34 sites that were evenly distributed in the region surrounding the Qinghai Lake (Figure 1). Information on the location of the sampling sites was acquired using a global positioning system (GPS). Groundwater samples were filtered using 0.45-μm nylon filters and were stored in 30- and 100-mL high-density polyethylene bottles for isotopic and chemical analyses, respectively. Electrical conductivity (EC) and pH of groundwater were measured in situ by a handheld meter. Stable isotopes were analyzed using the Los Gatos Research IWA-45-EP isotopic water analyzer. The measurement accuracy of δ^2H and $\delta^{18}O$ values was ±0.5 and ± 0.1‰, respectively. Hydrochemical parameters of groundwater samples were measured; these included TDS, TH, and the content of K^+, Na^+, Ca^{2+}, Mg^{2+}, CO_3^{2-}, HCO_3^-, SO_4^{2-}, Cl^-, and NO_3^- ions. The cations and anions were measured at Ludong University using ion chromatography (Dionex 600 and Dionex-500) and the repeated sampling error was 0.5–1% (2σ). Basic ions, CO_3^{2-} and HCO_3^-, were measured in situ using direct titration with phenolphthalein, methyl orange, and sulfuric acid.

The Piper diagram (Piper 1944) and the boomerang envelope model (Gibbs 1970) were used to reveal the hydrochemical characteristics and evolution of groundwater. In a Piper diagram, hydrogeochemical categorization of groundwater, river water, and lake water is carried out based on the major cations and anions present (Piper 1944). Gibbs (1970) analyzed the chemical composition of surface water samples from across the globe and classified the factors controlling the composition of water into three endmembers: rock weathering, atmospheric precipitation, and evaporation/crystallization (Machender et al. 2014). Groundwater quality was assessed according to the Chinese State Standards for drinking water (Chinese Ministry of Health 2006; Chinese General Administration of Quality Supervision 2017). According to these standards, the upper acceptable limits of pH, TDS, and TH are 8.5, 1000, and 450 mg/L, respectively, while that of Na^+, SO_4^{2-}, Cl^-, and NO_3^- content are 200, 250, 250, and 20 mg/L, respectively.

To analyze spatial characteristics, that is, water level, hydrochemistry, and stable isotope composition of groundwater in more detail, area of interest surrounding the lake was divided into four regions: east (G1-G11), south (G12-G20), west (G21-G29), and north (G30-G34) of the Qinghai Lake.

Results and Discussion

Stable Isotope Composition of Precipitation

The δ^2H values of precipitation ranged from −222.6 to −0.3‰ (with an average of −61.7‰), whereas the $\delta^{18}O$ values ranged from −30.5 to −0.8‰ (with an average of −9.3‰) (Figure 2). The range of δ^2H and $\delta^{18}O$ was consistent with previous research (Cui and Li 2014). Both δ^2H and $\delta^{18}O$ values were within the globally reported ranges for precipitation (δ^2H: −350 to +50‰, $\delta^{18}O$: −50 to +10‰) and the average ranges reported for China (δ^2H: −280.0 to +24.0‰, $\delta^{18}O$: −35.5 to +2.5‰) (IAEA 2001; Tian et al. 2001). The LMWL was simulated, and the results are shown in Figure 2: $\delta^2H = 7.80\ \delta^{18}O + 10.98$ VSMOW ($n = 104$, $R = 0.985$); it deviated slightly from the global meteoric water line (GMWL). The slope of LMWL was lower than that of the GMWL, while it was similar to the slopes observed previously for meteoric water lines in Lasa (7.90; Tian et al. 2001) and western China (7.56; Ma et al. 2009). This indicated that the precipitation processes in the basin are affected by below-cloud secondary evaporation (Liu et al. 2008; Gui et al. 2019) because humidity in the inland arid area is low, and raindrops undergo evaporation as they fall, causing isotope

Table 2
Information on water levels at 14 sites for groundwater surrounding the Qinghai Lake

No.	Sample	Elevation (m a.s.l.)	Depth Below Surface (m)	Relative Altitude (m)	Distance from Lake (km)	Hydraulic Gradient (‰)
1	G4	3249	0.85	8.48	5.57	1.52
2	G6	3243	3.00	−0.12	0.52	−0.24
3	G7	3246	3.00	3.48	0.54	6.40
4	G10	3250	3.70	6.23	2.70	2.31
5	G11	3256	4.35	12.13	2.73	4.44
6	G13	3365	2.30	122.91	2.85	43.13
7	G17	3253	2.65	11.13	0.97	11.47
8	G20	3249	2.90	6.06	1.35	4.50
9	G24	3246	2.18	3.83	4.77	0.80
10	G26	3281	3.50	37.46	17.63	2.12
11	G27	3316	3.52	72.84	32.00	2.28
12	G29	3242	3.70	−1.27	0.20	−6.20
13	G30	3270	10.87	19.79	5.38	3.68
14	G31	3300	4.00	56.85	11.39	4.99

Notes: Relative altitude: groundwater level relative to the water level of Qinghai Lake; Distance: between sample site and Qinghai Lake.

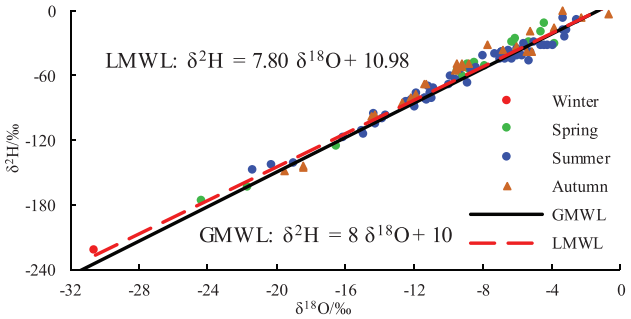

Figure 2. The relationship between δ^2H and $\delta^{18}O$ in precipitation of the Qinghai Lake Basin.

fractionation, and thus, a decrease in the LMWL slope (Araguas-Araguas et al. 1998; Cui and Li 2015a; Zhang and Wang 2016). Hydrogen and oxygen stable isotopes in precipitation were relatively enriched in summer and depleted in winter (Figure 2). The weighted means of $\delta^{18}O$ in spring, summer, autumn, and winter seasons were −9.5, −9.1, −9.5, and −23.8‰, respectively. This pattern was consistent with that of local temperatures, indicating that stable isotope composition in precipitation over the Qinghai Lake Basin is affected by temperature. Similar effects have been observed in Delingha, Urumqi, Zhangye (western China), and other arid regions in central Asia (Tian et al. 2001; Liu et al. 2008). The LMWL was slightly above the GMWL, indicating that the d-excess value of precipitation in the basin was relatively high (Kong et al. 2013). This suggested the occurrence of moisture loss from the continent as recycled precipitation due to low humidity (Pang et al. 2011, 2017).

Variation in the Levels of Groundwater Surrounding the Qinghai Lake

Due to some residents' wells being sealed, the groundwater level was investigated at only 14 sites among the 34 chosen sampling sites surrounding the Qinghai Lake (Table 2). The depth below surface of groundwater ranged from 0.85 to 10.87 m (mean = 3.97 m). The range of depth was similar to that reported in a previous study by Xiao et al. (2013; 0.9 to 8.2 m, mean = 3.80 m). However, the depth of groundwater could not reflect the direction of groundwater flow due to the different elevations of sampling sites. The difference of altitude between the groundwater level and the level of water in the Qinghai Lake was calculated at each sampling site (Table 2). This difference in altitude ranged from −1.27 to 122.91 m (mean = 25.70 m). The difference in altitude at most sites, excluding G6 and G29, constituted positive values (Table 2), indicating the groundwater level to be higher than the level of water in the Qinghai Lake; this indicated that most of the groundwater flowed into the lake. Based on the positive values of the difference in altitude of water levels (Table 2), average relative altitude was calculated for each of the four regions surrounding the lake. The average relative altitudes were found to be in the order of south > north > west > east with average values being 46.70, 38.32, 38.04, and 7.58 m, respectively.

The hydraulic gradient of each groundwater sample was calculated based on the relative altitude of groundwater levels and the distance between the sampling site and the Qinghai Lake (Table 2). The values thus obtained ranged from −6.20 to 43.14‰, with an average of 5.80‰. The average hydraulic gradient in the four regions was in the order of south > east > north > west with the values being 19.70, 4.6, 4.33, and 1.73‰, respectively, indicating that the driving force of groundwater at the south of Qinghai Lake was larger as compared to that in other regions. Lacustrine sediment terraces and faults are present along the south shore of Qinghai Lake, while other areas surrounding the lake are overlain by lacustrine and alluvial sediments. Groundwater is recharged by mountain runoff via infiltration across the alluvial and diluvial plains

(Xiao et al. 2012). Therefore, the distribution and variation of groundwater levels surrounding the Qinghai Lake is mainly attributable to geomorphology, terrain, groundwater aquifers, and fault characteristics (Jin et al. 2009; Xiao et al. 2012).

Stable Isotope Composition of Groundwater Surrounding the Qinghai Lake

The δ^2H values of groundwater in the vicinity of the Qinghai Lake ranged from −66.7 to −42.0‰ (mean = −51.4‰), while the $\delta^{18}O$ values ranged from −10.4 to −5.9‰ (mean = −8.0‰) (Figure 3). Both δ^2H and $\delta^{18}O$ values were within the isotope ranges measured in local precipitation samples (Figure 2, Figure 3). According to Figure 3, most of the isotope points of groundwater were present close to the LMWL; the LEL of groundwater was simulated as $\delta^2H = 6.08\ \delta^{18}O - 3.01$, where the slope of LEL (6.08) was lower than that of the LMWL (7.80). This indicated that groundwater in the vicinity of the Qinghai Lake was primarily recharged by local precipitation that had undergone varying degrees of evaporation before infiltration into the ground (Clark and Fritz 1997; Cui and Li 2014).

According to Table 1, the $\delta^{18}O$ content in groundwater lying to the east, south, west, and north of the Qinghai Lake ranged from −10.4 to −7.8‰, −9.0 to −6.6‰, −9.0 to −5.9‰, and −7.2 to −6.7‰, respectively, with average $\delta^{18}O$ values of −8.6, −8.0, −7.8, and −6.9‰, respectively, indicating that groundwater was recharged by precipitation at different altitudes (Gremillion and Wanielista 2000; Cui and Li 2014). The average $\delta^{18}O$ content in groundwater from the different regions was in the order of $\delta^{18}O_{North} > \delta^{18}O_{West} > \delta^{18}O_{South} > \delta^{18}O_{East}$. There are two possible scenarios that could explain this trend: one possibility is that the groundwater lying to the east of the Qinghai Lake could have a relatively higher recharge altitude than other regions; the other possibility is that the groundwater present to the north of the Qinghai Lake could have undergone stronger evaporation than water in other regions surrounding the lake before infiltration. The LEL slope of groundwater lying to the east, south, west, and north of the Qinghai Lake was 7.25, 4.48, 4.22, and 3.94, respectively (Table 3; Figure 3), indicating that the degree of evaporation of groundwater before infiltration was in the order of north > west > south > east (Weyhenmeyer et al. 2002; Dogramaci et al. 2012). Therefore, the average $\delta^{18}O$ values corresponded with the second possible scenario. As compared to the east and south regions, the north and west regions that were overlain by alluvial and lacustrine sediments had a relatively flat terrain with a low hydraulic gradient (Figure 1, Table 2) due to which surface water flowed slowly and took relatively longer to infiltrate (Buda et al. 2013). Owing to the longer time required for infiltration of surface water, the degree of evaporation before infiltration was greater as well (Weyhenmeyer et al. 2002; Buda et al. 2013). These patterns suggest that the degree of evaporation of groundwater in the west and north was higher than that in the south and east of the Qinghai Lake. To find the initial stable isotope content in groundwater and to eliminate the influence of evaporation, intersections between the LMWL and the LEL of groundwaters in each region were calculated; these values are presented in Table 3 (Clark and Fritz 1997; Cui and Li 2014). The initial isotope content in groundwater was in the order of $\delta_{North} > \delta_{West} > \delta_{South} > \delta_{East}$, with the values being −7.30, −8.09, −8.11, and −11.14‰, respectively (Table 3). Considering the effect of altitude on $\delta^{18}O$ content in precipitation, the average recharge altitude of groundwater in the four regions was in the order of east > south > west > north (Cui and Li 2014).

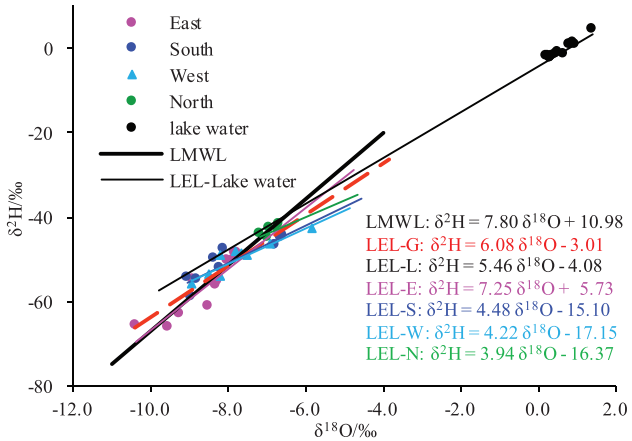

Figure 3. Characteristics of the stable isotope composition of groundwater in the four regions.

As shown in Table 1, the $\delta^{18}O$ content at G29 (−5.9‰) was higher than that at other sites of groundwater collection and lower than that in lake water (average $\delta^{18}O$: 1.6‰; Cui et al. 2016). Furthermore, the water level at G29 (relative altitude = −1.27 m, hydraulic gradient = −6.20‰) was lower than the level of water in the Qinghai Lake (Table 2), suggesting that G29 may be recharged by lake water. The water level at G6 (relative altitude = −0.12 m) was also lower than the level of water in the Qinghai Lake (Table 2), but the $\delta^{18}O$ content in groundwater at this site (−9.0‰) was relatively lower (Table 1). There are two possible reasons for both the water level and $\delta^{18}O$ content being lower at G6. One is the existence of a weak hydraulic connection between G6 and lake water due to the slightly negative hydraulic gradient (−0.24‰); the second possibility is that groundwater at G6 was recharged by fissure water that was relatively depleted in isotopes because G6 was located in a fault zone of the southern margin of the Zhongqilian Massif. Overall, groundwater surrounding the Qinghai Lake was primarily recharged from local precipitation at different altitudes.

Hydrochemical Characteristics of Groundwater Surrounding the Qinghai Lake

Groundwater pH ranged from 7.54 to 8.36 with a mean value of 8.04, indicating that groundwater in the vicinity of the Qinghai Lake was slightly alkaline. The ranges of groundwater pH were similar to the pH ranges

Table 1
Stable Isotope and Hydrochemical Compositions of Groundwater Surrounding the Qinghai Lake

Sample	$\delta^{18}O$ (‰)	$\delta^{2}H$ (‰)	Ca^{2+} (mg/L)	Mg^{2+} (mg/L)	Na^{+} (mg/L)	K^{+} (mg/L)	HCO_3^{-} (mg/L)	Cl^{-} (mg/L)	SO_4^{2-} (mg/L)	NO_3^{-} (mg/L)	TDS (mg/L)	EC (ms/cm)	TH (mg/L)	pH	Elevation (m)
G1	−8.29	−55.52	70.18	38.68	179.52	4.41	223.12	103.95	152.33	8.68	772.18	1.60	334.54	8.01	3263
G2	−7.78	−48.81	40.69	13.75	10.06	1.33	201.92	4.45	12.68	5.34	284.87	0.39	158.23	8.14	3271
G3	−7.84	−48.89	42.67	16.83	9.03	1.85	215.04	5.57	14.22	4.94	305.20	0.42	175.87	8.14	3245
G4	−7.85	−50.69	259.30	110.59	193.86	34.85	418.98	294.79	207.67	100.88	1520.05	3.27	1102.97	7.54	3249
G5	−8.03	−50.77	45.84	17.64	35.99	2.15	258.46	11.40	20.41	4.92	391.89	0.57	187.13	8.19	3219
G6	−9.26	−63.35	30.37	26.71	371.34	11.51	360.43	143.40	136.77	5.75	1092.44	2.05	185.84	8.30	3243
G7	−8.51	−61.60	46.72	31.59	103.79	5.51	259.47	54.02	50.96	14.16	552.06	1.01	246.77	7.96	3246
G8	−9.57	−66.64	36.50	14.68	13.32	3.51	181.73	10.16	9.41	8.06	269.30	0.40	151.59	8.29	3215
G9	−8.34	−56.51	56.13	11.29	25.33	2.33	224.13	12.31	14.52	10.83	346.02	0.55	186.65	8.23	3292
G10	−10.41	−66.18	52.02	52.13	114.31	50.97	342.25	82.84	59.00	19.15	753.52	1.37	344.57	8.23	3250
G11	−8.89	−55.19	113.40	21.52	176.33	3.80	326.10	115.34	45.01	53.82	801.50	1.76	371.83	7.92	3256
G12	−9.03	−54.61	45.53	12.00	10.94	2.13	202.93	7.36	10.24	4.76	291.12	0.42	163.13	8.16	3195
G13	−8.79	−55.04	55.35	16.37	12.27	3.27	266.53	6.56	10.82	4.85	371.17	0.50	205.64	8.04	3365
G14	−8.22	−52.24	92.02	21.77	64.64	3.19	344.27	28.78	58.35	8.15	613.01	0.99	319.44	8.12	3221
G15	−8.96	−59.39	63.48	27.76	50.75	4.42	241.29	55.54	19.21	6.10	462.45	0.87	272.85	8.36	3212
G16	−6.77	−46.96	71.95	99.28	101.32	5.76	433.12	53.95	66.14	74.46	843.44	1.69	588.48	8.14	3250
G17	−6.65	−45.03	56.19	64.30	96.12	1.90	410.91	45.43	40.02	17.88	723.80	1.28	405.10	7.89	3253
G18	−6.57	−44.52	60.14	13.87	13.93	2.44	247.35	11.76	10.87	6.17	360.37	0.62	207.30	8.10	3228
G19	−8.38	−50.06	85.09	23.60	35.06	4.19	347.30	22.26	22.71	15.76	540.20	0.83	309.70	7.65	3209
G20	−8.13	−48.01	78.73	23.94	30.58	4.07	327.11	20.26	22.36	13.35	507.06	0.79	295.22	8.04	3249
G21	−8.20	−49.16	61.81	27.74	46.49	2.61	276.63	31.15	22.37	10.81	468.80	0.84	268.58	8.09	3226
G22	−7.81	−48.17	78.45	14.30	15.21	0.71	356.39	5.23	8.14	4.63	478.42	0.62	254.83	7.74	3216
G23	−7.69	−48.94	48.68	24.99	72.62	2.60	328.12	27.00	20.02	7.68	524.03	0.78	224.49	8.14	3202
G24	−8.21	−54.38	72.97	29.07	77.60	6.76	296.82	40.50	33.56	26.71	557.29	1.10	301.95	7.83	3246
G25	−7.54	−49.24	149.49	86.51	308.21	2.24	680.47	108.71	161.78	117.64	1497.42	2.75	729.58	7.72	3199
G26	−6.94	−46.37	65.27	24.06	62.83	2.70	298.84	34.17	29.25	7.32	517.12	0.84	262.09	8.05	3281
G27	−8.98	−56.14	79.63	24.91	22.16	2.90	330.14	12.51	26.16	4.60	498.41	0.78	301.43	7.81	3316
G28	−8.49	−53.61	80.18	32.79	71.29	3.34	334.18	45.42	37.51	12.26	604.71	1.05	335.26	8.12	3307
G29	−5.86	−42.82	39.51	58.42	177.91	6.56	477.54	59.42	51.77	14.18	885.04	1.41	339.24	8.25	3242
G30	−6.96	−45.23	69.84	36.38	77.52	2.86	347.30	36.58	33.87	6.64	613.29	1.02	324.20	8.12	3270
G31	−6.68	−43.18	56.79	40.10	60.23	2.22	340.24	24.44	28.40	7.75	562.35	0.88	306.97	8.25	3300
G32	−6.70	−41.99	72.23	31.27	45.93	4.20	353.36	20.61	27.47	10.12	571.94	0.89	309.13	7.55	3239
G33	−7.20	−44.40	55.72	24.91	49.06	2.64	262.50	26.47	28.47	7.96	459.70	0.79	241.75	7.94	3259
G34	−6.93	−42.85	30.80	20.76	21.48	2.13	161.54	10.79	16.65	5.24	272.08	0.46	162.42	8.35	3265

Table 3
The Evaporation Line of Groundwater in Four Regions Surrounding the Qinghai Lake

LEL Types	Equations	Initial $\delta^{18}O$ (‰)	*n*	*R*	*P*
East of Qinghai Lake (East-LEL)	$\delta^{2}H = 7.25\delta^{18}O + 5.73$	−11.14	11	0.901	<0.001
South of Qinghai Lake (South-LEL)	$\delta^{2}H = 4.48\delta^{18}O - 15.10$	−8.11	9	0.896	<0.001
West of Qinghai Lake (West-LEL)	$\delta^{2}H = 4.22\delta^{18}O - 17.15$	−8.09	9	0.926	<0.001
North of Qinghai Lake (North-LEL)	$\delta^{2}H = 3.94\delta^{18}O - 16.37$	−7.30	5	0.669	—

of river water (from 7.60 to 8.55) in the Qinghai Lake Basin (Jin et al. 2010). The TDS content and EC values of most of the groundwater samples, excluding G4, G6, and G29, ranged from 269 to 885 mg/L and from 0.39 to 1.76 mS/cm with average values of 523 mg/L and 0.89 mS/cm, respectively. The TDS content and EC of groundwater were relatively higher as compared to that of river water in the basin (mean values of 341.79 mg/L and 0.17 mS/cm, respectively) (Cui and Li 2015b). Our results indicated that the water-rocks interaction was stronger in case of groundwater than in case of river water. Except for G1, G4, G6, G7, G10, G11, G23, G25, and G29, the hydrochemical type of most of the groundwater samples was Ca-Mg-HCO_3 (Figure 4). Among other ions, the concentrations of Mg^{2+} and Ca^{2+} were relatively high, accounting for more than 60% of the cation content in groundwater surrounding the lake. Furthermore, our findings suggested that the hydrochemistry of groundwater may primarily be controlled by carbonate dissolution.

The hydrochemical types of groundwater collected from G1, G4, G6, G25, and G29 were Na-Cl-SO_4, Ca-Mg-Cl, Na-Cl-CO_3, Na-Ca-HCO_3, and Na-Mg-HCO_3,

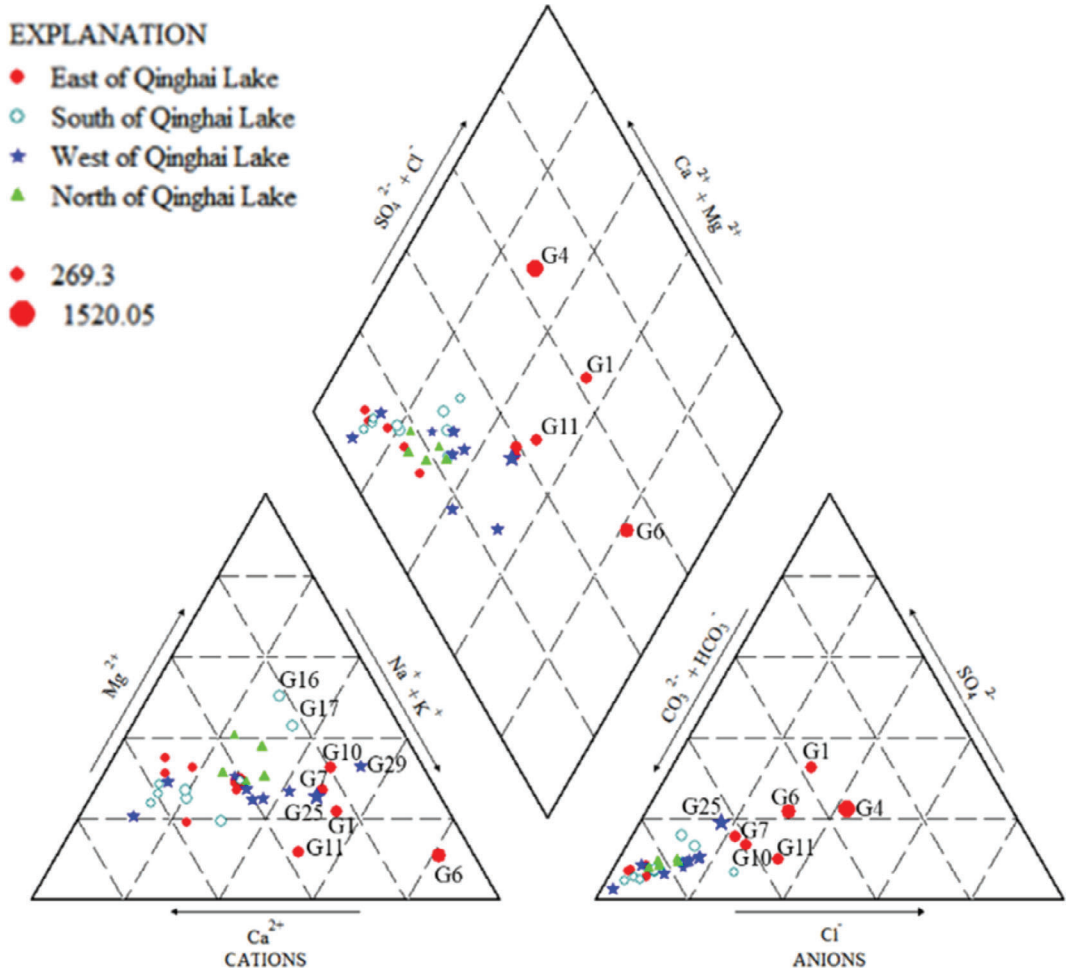

Figure 4. Ternary plots of cations and anions in groundwater surrounding the Qinghai Lake.

respectively (Figure 4). There could be two possible reasons for the high ion concentrations and TDS content in groundwater at these sites; first: a relatively long flow path, which could increase the time of interaction between rocks and water, increasing the TDS content in groundwater as well, and second: recharge of groundwater by lake water having high ion concentrations and TDS content.

The altitude of water level at G29 (−1.27 m) was lower than the level of water in the Qinghai Lake; G29 was located very close to the Qinghai Lake at a distance of only 0.20 km (Table 1, Figure 1). The $\delta^{18}O$ content in groundwater at G29 (−5.9‰) was higher than that in other groundwater samples, indicating that there may have been a strong hydraulic contact between the lake and G29, that is, groundwater at G29 was partially recharged by the Qinghai Lake water (Cui et al. 2016). The $\delta^{18}O$ content in groundwater from G1 (−8.3‰) and G6 (−9.0‰) was relatively lower than that in groundwater from other sites surrounding the Qinghai Lake (Table 1); G1 and G6 are located in the fault zone of the southern margin of the Zhongqilian Massif, indicating that they are recharged partially by fissure water that is relatively depleted in isotope content. The relative altitude of water levels at G4 and G25 was higher than the level of water in the Qinghai Lake; the $\delta^{18}O$ content in groundwater from G4 (−7.9‰) and G25 (−7.5‰) was slightly higher (Table 2), indicating that groundwater at these sites was not recharged by the lake water. High concentrations and TDS content can be attributed to intense evaporation before infiltration or a high content of dissolved solids (Xiao et al. 2012; Cui and Li 2014). Furthermore, G1, G4, G6, G25, and G29 were all distributed to the east and west of the Qinghai Lake, suggesting that the recharge sources of groundwater in the east and west of the lakes were relatively complex.

As shown in Figure 5, all samples fell within the evolutionary path from "Rock dominance" to "Ocean" (Gibbs 1970; Machender et al. 2014), indicating that the hydrochemical composition of groundwater surrounding the lake was primarily dominated by rock weathering. This finding is corroborated by previous studies that reported rock weathering and ion exchange to be the major geochemical processes responsible for the occurrence of solutes in groundwater in the Qinghai Lake Basin (Xiao et al. 2012; Cui and Li 2014). Relatively higher concentrations of Na^+ and Cl^- in some groundwater samples were attributable to evaporite dissolution (Xu et al. 2010) or to a long migration path of groundwater with strong water-rock interaction (Cui and Li 2014).

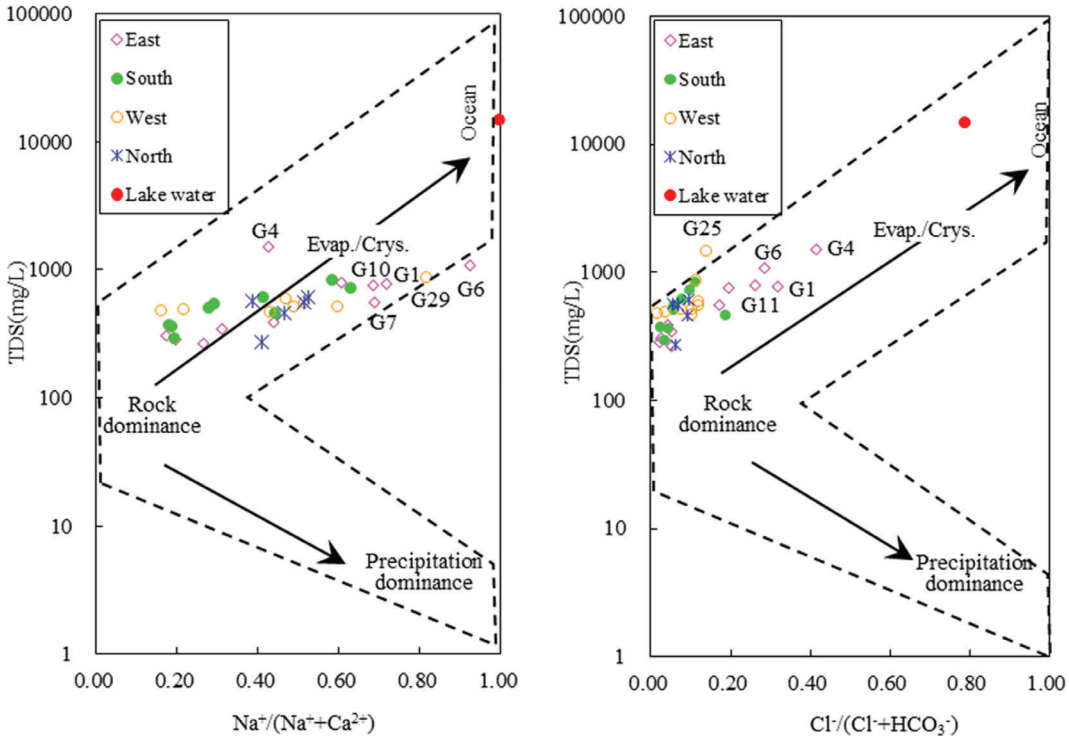

Figure 5. Plots of major ions within the Gibbs boomerang model for groundwater and lake water.

Evaluation of Groundwater Quality

High concentrations of some ions in drinking water can be harmful to human health; these ions include Na^+, Cl^-, NO_3^-, and SO_4^{2-} among others (Wasana et al. 2016, 2017; Nixdorf et al. 2017). For example, high concentrations of NO_3^- in drinking water could result in Fe-rich hemoglobin, hypertension, and birth defects, while an excess of SO_4^{2-} may cause diarrhea, dehydration, and weight loss (Ho et al. 2011; Jones et al. 2016). As presented in Table 1, most of the groundwater samples that were within the standards for drinking water with respect to all indices were slightly and moderately hard fresh water. However, TDS content in groundwater from G4 mg/L), G6, and G25 was higher than the upper acceptable limit of 1000 mg/L (Table 1). Concentration of Na^+ in groundwater from G6 and G25 was higher than the standard of 200 mg/L. Concentration of Cl^- in groundwater from G4 was higher than the standard of 250 mg/L. Concentration of NO_3^- in groundwater from G4, G11, G16, G24, and G25 was higher than the permissible concentration of 20 mg/L (Table 1). These observations indicated that groundwater collected from locations, G4, G6, G11, G16, G24, and G25, exceeds the current drinking standards and is unsuitable for drinking (Ho et al. 2011; Wasana et al. 2016, 2017). The water levels, hydrochemistry, and isotope compositions of groundwater, high TDS content, and concentrations of ions in groundwater from locations, G4 and G25, were due to strong evaporation or an excess of dissolved solids (Xiao et al. 2012; Cui and Li 2014). High TDS content and concentrations of ions in groundwater from location G6 were attributed to the recharging source, that was fissure water in this case (Xu et al. 2010; Cui and Li 2014). These observations highlight the influence of natural factors on groundwater quality, such as geomorphology, terrain, groundwater aquifers, fault types, etc. (Jin et al. 2009).

In general, if the concentration of nitrogen present in the form of NO_3^- is higher than 3.0 mg/L, it can be inferred that the water body has been influenced by human activities (Babiker et al. 2004). As presented in Table 1, the concentration of NO_3^- in all groundwater samples was higher than 4.60 mg/L, indicating that the groundwater in the vicinity of the lake was affected by human activities, especially in locations, G4, G11, G16, G24, and G25; some locations had NO_3^- concentrations even higher than the upper acceptable limit of 20 mg/L for NO_3^-. The Qinghai Lake basin, lying in the Northeast Qinghai-Tibet Plateau, is a sparsely populated region with only a few events of mineral exploitations in the past and a small number of large-scale factories (Li et al. 2018). The region surrounding the Qinghai Lake is important for ecological tourism and animal husbandry in the Qinghai Province as well (Li et al. 2018). Therefore, the main sources of nitrate (NO_3^-) in groundwater here are animal feces and sewage. To further identify the source of NO_3^- in groundwater surrounding the lake, relationship trends between NO_3^- and Cl^- in groundwater were analyzed (Figure 6). Ratio analysis of major ions in groundwater, such as NO_3^-/Cl^-, SO_4^{2-}/Cl^-, and Cl^-/Br^-, can help determine the nature of pollution sources and migration processes of pollutants (Chen et al. 2009; Murgulet and Tick 2013). According to Figure 6, there was a positive correlation between NO_3^- and Cl^- ions in groundwater

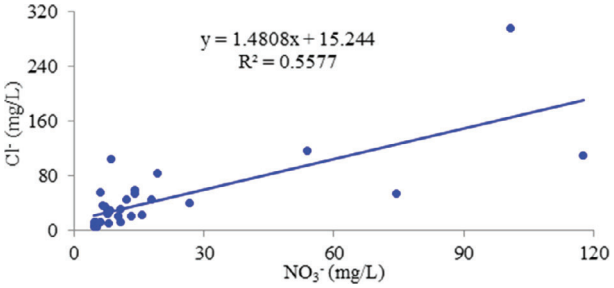

Figure 6. Relationship between NO_3^- and Cl^- in groundwater surrounding the Qinghai Lake.

($n = 34$, $P < 0.001$, $R = 0.747$), suggesting that the NO_3^- in groundwater mainly originated from animal feces and sewage that could be attributed to livestock breeding activities surrounding the Qinghai Lake.

Overall, the groundwater surrounding the Qinghai Lake was primarily recharged from precipitation over the basin, while hydrochemistry and isotope composition of groundwater were mainly controlled by initial precipitation and dissolution of surrounding rocks during runoff; this dissolution was, in turn, largely controlled by groundwater aquifers, fault type, terrain, and geomorphology (Xiao et al. 2012; Cui and Li 2014). The influence of livestock manure and wastewater on groundwater quality surrounding the lake cannot be ignored. Concentrations of some ions in the east and west of the Qinghai Lake were recorded to exceed the corresponding upper acceptable limits for drinking water. These observations suggest that groundwater pollution in areas practicing animal husbandry in the Qinghai-Tibet Plateau is significant despite rates of industrial and urbanization being relatively low in the plateau, and thus, needs mitigation measures (Wang et al. 2014). Therefore, scientific planning, engineering, and management of livestock manure and wastewater discharge in regions practicing animal husbandry is crucially and urgently requited to not only provide water resources that are safe for drinking but for the sustainable development of the environment of the Qinghai-Tibet Plateau as well.

Conclusions

This study investigated the water level, hydrochemistry, and stable isotope composition of groundwater surrounding the Qinghai Lake to reveal its recharge sources, hydrochemical evolution, and water quality. The LMWL was $\delta^2H = 7.80\ \delta^{18}O + 10.98$, indicating that precipitation was affected by below-cloud secondary evaporation and continental moisture recycle. Most of the points of groundwater collection lay close to the LMWL, where the slope of the LEL was smaller than that of the LMWL. Groundwater was slightly alkaline and was primarily recharged from local precipitation at different altitudes in the basin that had undergone varying degrees of evaporation before infiltration. The hydrochemical type of most of the groundwater samples was Ca-Mg-HCO_3, where the hydrochemistry was primarily controlled by carbonate dissolution. The recharge sources of groundwater in the east and west regions were relatively complex.

Most of the groundwater samples that satisfied the standards for drinking water in all indices were slightly and moderately hard fresh water. However, the groundwater from locations, G4 (TDS, Cl^-, and NO_3^-), G6 (TDS and Na^+), G11 (NO_3^-), G16 (NO_3^-), G24 (NO_3^-), and G25 (TDS, Na^+, and NO_3^-), exceeded the current drinking standards and was unsuitable for drinking. Overall, the impacts of livestock manure and wastewater on groundwater quality cannot be ignored surrounding the lake. Scientific planning, engineering, and management of livestock manure and wastewater discharge from animal husbandry is a crucial and urgent need in the Qinghai-Tibet Plateau to not only provide safe water resources for drinking purposes but for the sustainable development of the region as well.

Acknowledgments

The study was supported by the National Natural Science Foundation of China (41730854, 41877157); the Project supported by State Key Laboratory of Loess and Quaternary Geology (SKLLQG1904); the Science and technology support plan for Youth Innovation of colleges and universities of Shandong (2019KJH009); the Natural Science Foundation of Shandong Province (ZR2019BD005; ZR2019MD040); the Key Research and Development Plan of Shandong Province (2018GSF117021); the Science and technology program of colleges and universities of Shandong (J17KA192); and the Project supported by State Key Laboratory of Earth Surface Processes and Resource Ecology (2017-KF-15). We are grateful to Christopher Eastoe and Melissa Lenczewski whose comments improved the quality of this manuscript.

Authors' Note

The authors do not have any conflicts of interest.

References

Alley, W.M., Healy, R.W., LaBaugh, J.W. & Reilly, T.E. (2002) Flow and Storage in Groundwater Systems. *Science* , 296(5575), 1985–1990.

Araguas-Araguas, L., K. Froehlich, and K. Rozanski. 1998. Stable isotope composition of precipitation over southeast Asia. *Journal of Geophysical Research-Atmospheres* 103, no. D22: 28721–28742.

Babiker, I.S., M.A.A. Mohamed, H. Teraoa, K. Kato, and K. Ohta. 2004. Assessment of groundwater contamination by nitrate leaching from intensive vegetable cultivation using geographical information system. *Environment International* 29, no. 8: 1009–1017.

Bicalho, C.C., C. Batiot-Guilhe, J.D. Taupin, N. Patris, S. Van Exter, and H. Jourde. 2019. A conceptual model for groundwater circulation using isotopes and geochemical tracers coupled with hydrodynamics: A case study of the Lez karst system, France. *Chemical Geology* 528: 118442.

Buda, A.R., P.J.A. Kleinman, G.W. Feyereisen, D.A. Miller, P.G. Knight, P.J. Dorhan, and R.B. Bryant. 2013. Forecasting runoff from Pennsylvania landscapes. *Journal of Soil and Water Conservation* 68, no. 3: 185–198.

Chang, J., and G.X. Wang. 2010. Major ions chemistry of groundwater in the arid region of Zhangye Basin, northwestern China. *Environmental Earth Sciences* 61, no. 3: 539–547.

Chang, H., Z.D. Jin, and Z.S. An. 2009. Sedimentary evidences of the uplift of the Qinghai Nanshan (the Mountains South to Qinghai Lake) and its implication for structural evolution of the Lake Qinghai Gonghe Basin. *Geological Review* 55, no. 1: 49–57 (in Chinese).

Chen, F.J., G.D. Jia, and J.Y. Chen. 2009. Nitrate sources and watershed denitrification inferred from nitrate dual isotopes in the Beijiang River, south China. *Biogeochemistry* 94, no. 2: 163–174.

Chinese General Administration of Quality Supervision, (2017) Standard for Groundwater Quality. Beijing: Standards Press of China (in Chinese),

Chinese Ministry of Health, (2006) Standards for Drinking Water Quality. Beijing: Standards Press of China (in Chinese),

Clark, I.D., and P. Fritz. 1997. *Environmental Isotopes in Hydrogeology*. New York: Lewis Publishers.

Cui, B.L., and X.Y. Li. 2014. Characteristics of stable isotope and hydrochemistry of the groundwater around Qinghai Lake, NE Qinghai-Tibet plateau, China. *Environmental Earth Sciences* 71, no. 3: 1159–1167.

Cui, B.L., and X.Y. Li. 2015a. Stable isotopes reveal sources of precipitation in the Qinghai Lake Basin of the northeastern Tibetan Plateau. *Science of the Total Environment* 527-528: 26–27.

Cui, B.L., and X.Y. Li. 2015b. Characteristics of stable isotopes and hydrochemistry of river water in the Qinghai Lake Basin, northeast Qinghai-Tibet Plateau, China. *Environment and Earth Science* 73, no. 8: 4251–4263.

Cui, B.L., X.Y. Li, and X.H. Wei. 2016. Isotope and hydrochemistry reveal evolutionary processes of lake water in Qinghai Lake. *Journal of Great Lakes Research* 42, no. 3: 580–587.

Dogramaci, S., G. Skrzypek, W. Dodson, and P.F. Grierson. 2012. Stable isotope and hydrochemical evolution of groundwater in the semi-arid Hamersley Basin of subtropical northwest Australia. *Journal of Hydrology* 475: 281–293.

Edmunds, W.M. 2009. Geochemistry's vital contribution to solving water resource problems. *Applied Geochemistry* 24, no. 6: 1058–1073.

Gibbs, R.J. 1970. Mechanisms controlling world water chemistry. *Science* 170: 1088–1090.

Gibson, J.J., T.W.D. Edwards, S.J. Birks, N.A. St Amour, W.M. Buhay, P. McEachern, B.B. Wolfe, and D.L. Peters. 2005. Progress in isotope tracer hydrology in Canada. *Hydrological Processes* 19: 303–327.

Gleeson, T., Y. Wada, M.F.P. Bierkens, and L.P.H. van Beek. 2012. Water balance of global aquifers revealed by groundwater footprint. *Nature* 488: 197–200.

Gleeson, T., K.M. Befus, and S. Jasechko. 2016. The global volume and distribution of modern groundwater. *Nature Geoscience* 9, no. 2: 161–167.

Goldin, T. 2016. Groundwater: India's drought below ground. *Nature Geoscience* 9, no. 2: 98.

Gremillion, P., and M. Wanielista. 2000. Effects of evaporative enrichment on the stable isotope hydrology of a Central Florida (USA) river. *Hydrological Processes* 14, no. 8: 1465–1484.

Gui, J., Z.S. Li, Q. Feng, W. Wei, Y.G. Li, Y.M. Lv, R.F. Yuan, and B.J. Zhang. 2019. Space-time characteristics and environmental significance of the stable isotopes in precipitation in the Gulang River basin. *Environmental Sciences* 40, no. 1: 149–156 (in Chinese).

Ho, C.K., Y.H. Yang, and C.Y. Yang. 2011. Nitrates in drinking water and the risk of death from brain cancer: Does hardness in drinking water matter? *Journal of Toxicology and Environmental Health-Part A-Current Issues* 74, no. 12: 747–756.

IAEA/WMO. 2001. Global Network for Isotopes in Precipitation. The Global Network for Isotopes in Precipitation Database. http://isohis.iaea.org (accessed December 24, 2019).

Jin, Z.D., J.M. Yu, S.M. Wang, F. Zhang, Y.W. Shi, and C.F. You. 2009. Constraints on water chemistry by chemical weathering in the Lake Qinghai catchment, northeastern Tibetan Plateau (China): Clues from Sr and its isptppic geochemistry. *Hydrogeology Journal* 17, no. 8: 2037–2048.

Jin, Z.D., S.M. Wang, F. Zhang, and Y.W. Shi. 2010. Weathering, Sr fluxes, and controls on water chemistry in the Lake Qinghai catchment, NE Tibetan Plateau. *Earth Surface Processes and Landforms* 35, no. 9: 1057–1070.

Jones, R.R., P.J. Weyer, C.T. Dellavalle, M. Inoue-Choi, K. Anderson, K.P. Cantor, S. Krasner, K. Robien, L.E.B. Freeman, D. Silverman, and M.H. Ward. 2016. Nitrate from drinking water and diet and bladder cancer among postmenopausal women in Iowa. *Environmental Health Perspectives* 124, no. 11: 1751–1758.

Kong, Y.L., Z.H. Pang, and K. Froehlich. 2013. Quantifying recycled moisture fraction in precipitation of an arid region using deuterium excess. *Tellus Series B: Chemical and Physical Meteorology* 65B: 19251.

Li, P.Y., H. Qian, J.H. Wu, Y.Q. Zhang, and H.B. Zhang. 2013. Major ion chemistry of shallow groundwater in the Dongsheng coalfield, Ordos Basin, China. *Mine Water and the Environment* 32, no. 3: 195–206.

Li, X.Y., Y.J. Ma, and Y.M. Huang. 2018. *Study on Eco-Hydrological Process and Water Balance in Qinghai Lake Basin*. Beijing, China: Science Press (in Chinese).

Li, N., H. Zhou, Z. Wen, and H. Jakada. 2019. Formation mechanism and mixing behaviour of Nanyang thermal spring, Xingshan County of Hubei Province, central China. *Hydrogeology Journal* 27, no. 8: 2933–2953.

Liu, J.R., X.F. Song, G.F. Yuan, X.M. Sun, X. Liu, F. Chen, Z.M. Wang, and S.Q. Wang. 2008. Characteristics of $\delta^{18}O$ in precipitation over Northwest China and its water vapor sources. *Acta Geographica Sinica* 63, no. 1: 12–22 (in Chinese).

Liu, F., X.F. Song, L.H. Yang, D.M. Han, Y.H. Zhang, Y. Ma, and H.M. Bu. 2015. The role of anthropogenic and natural factors in shaping the geochemical evolution of groundwater in the Subei Lake basin, Ordos energy base, Northwestern China. *Science of the Total Environment* 538: 327–340.

Ma, J., Z. Ding, W.M. Edmunds, J.B. Gates, and T.M. Huang. 2009. Limits to recharge of groundwater from Tibetan plateau to the Gobi desert, implications for water management in the mountain front. *Journal of Hydrology* 364, no. 1–2: 128–141.

Machender, G., R. Dhakate, M.N. Reddy, and I.P. Reddy. 2014. Hydrogeochemical characteristics of surface water (SW) and groundwater (GW) of the Chinnaeru River basin, northern part of Nalgonda District, Andhra Pradesh, India. *Environmental Earth Sciences* 71, no. 6: 2885–2910.

Murgulet, D., and G.R. Tick. 2013. Understanding the sources and fate of nitrate in a highly developed aquifer system. *Journal of Contaminant Hydrology* 155: 69–81.

Nixdorf, E., Y.Y. Sun, M. Lin, and O. Kolditz. 2017. Development and application of a novel method for regional assessment of groundwater contamination risk in the Songhua River Basin. *Science of the Total Environment* 605: 598–609.

Oki, T., and S. Kanae. 2006. Global hydrological cycles and world water resources. *Science* 313, no. 5790: 1068–1072.

Pang, Z.H., Y.L. Kong, K. Froehlich, T.M. Huang, L.J. Yuan, Z.Q. Li, and F.T. Wang. 2011. Processes affecting isotopes in precipitation of an arid region. *Tellus Series B: Chemical and Physical Meteorology* 63, no. 3: 352–359.

Pang, Z.H., Y.L. Kong, J. Li, and J. Tian. 2017. An isotopic geoindicator in the hydrological cycle. *Procedia Earth and Planetary Science* 17: 534–537.

Piper, A.M. 1944. A graphic procedure in the geochemical interpretation of water-analysis. *Transactions of the American Geophysical Union* 25, no. 6: 914–923.

Postel, S.L., G.C. Daily, and P.R. Ehrlich. 1996. Human appropriation of renewable fresh water. *Science* 271, no. 5250: 785–788.

Qiu, J. 2010. China faces up to groundwater crisis. *Nature* 466: 308.

Raghavendra, N.S., and P.C. Deka. 2015. Sustainable development and Management of Groundwater Resources in mining affected areas: A review. *Procedia Earth and Planetary Science* 11: 598–604.

Rodell, M., I. Velicogna, and J.S. Famiglietti. 2009. Satellite-based estimates of groundwater deletion in India. *Nature* 460, no. 7258: 999–1002.

Sun, D.P., Y. Tang, Z.Q. Xu, and Z.M. Han. 1991. A preliminary investigation on chemical evolution of the Lake Qinghai water, China. *Chinese Science Bulletin* 37, no. 3: 221–225.

Tang, L.Y., X.F. Duan, F.J. Kong, F. Zhang, Y.F. Zheng, Z. Li, Y. Mei, Y.W. Zhao, and S.J. Hu. 2018. Influences of climate change on area variation of Qinghai Lake on Qinghai-Tibetan Plateau since 1980s. *Scientific Reports* 8: 7331.

Taucare, M., L. Daniele, B. Viguier, A. Vallejos, and G. Arancibia. 2020. Groundwater resources and recharge processes in the Western Andean Front of Central Chile. *Science of the Total Environment* 722: 137824.

Tian, L.D., T.D. Yao, W.Z. Sun, M. Stievenard, and J. Jouzel. 2001. Relationship between δD and δ^{18}O in precipitation from north to south of the Tibetan Plateau and moisture cycling. *Science in China* 44, no. 9: 789–796 (in Chinese).

Tweed, S., S. Massuel, J.L. Seidel, K. Chhuon, S. Lun, K.E. Eang, J.P. Venot, G. Belaud, M. Babic, and M. Leblanc. 2020. Seasonal influences on groundwater arsenic concentrations in the irrigated region of the Cambodian Mekong Delta. *Science of the Total Environment* 728: 138598.

Van Loon, A.F., T. Gleeson, J. Clark, A.I.J.M. Van Dijk, K. Stahl, J. Hannaford, G. Di Baldassarre, A.J. Teuling, L.M. Taallaksen, R. Uijlenhoet, D.M. Hannah, J. Sheffield, M. Svoboda, B. Verbeuren, T. Wangener, S. Rangecroft, N. Wanders, and H.A.J. Van Lanen. 2016. Drought in the Anthropocene. *Nature Geoscience* 9, no. 2: 89–91.

Wang, X.M., Y.W. Chai, C. Cheng, and Y.J. Bu. 2014. Impact assessment of ecological service value in the rapid urbanization area of Qinghai-Tibet plateau: A case study of Xining. *China Population*. *Resources and Environment* 24, no. 5: 435–439.

Wasana, H.M.S., D. Aluthpatabendi, W.M.T.D. Kularatne, P. Wijekoon, R. Weerasooriya, and J. Bandara. 2016. Drinking water quality and chronic kidney disease of unknown etiology (CKDu): Synergic effects of fluoride, cadmium and hardness of water. *Environmental Geochemistry and Health* 38, no. 1: 157–168.

Wasana, H.M.S., G.D.R.K. Perera, P.D. Gunawardena, P.S. Fernando, and J. Bandara. 2017. WHO water quality standards vs synergic effect(s) of fluoride, heavy metals and hardness in drinking water on kidney tissues. *Scientific Reports* 7: 42516.

Weyhenmeyer, C.E., S.J. Burns, H.N. Waber, and P.G. Macumber. 2002. Isotope study of moisture sources, recharge areas, and groundwater flow paths within the eastern Batinah coastal plain, Sultanate of Oman. *Water Resources Research* 38, no. 10: 1184–1206.

Xiao, J., Z.D. Jin, F. Zhang, and J. Wang. 2012. Solute geochemistry and its sources of the groundwater's in the Qinghai Lake Catchment, NW China. *Journal of Asian Earth Science* 52: 21–30.

Xiao, J., Z.D. Jin, and F. Zhang. 2013. Geochemical and isotopic characteristics of shallow groundwater within the Lake Qinghai catchment, NE Tibetan Plateau. *Quaternary International* 313-314: 62–73.

Xin, H. 2008. A green fervor sweeps the Qinghai-Tibetan Plateau. *Science* 321, no. 5889: 633–635.

Xu, H., Z. Hou, Z. An, X. Liu, and J. Dong. 2010. Major ion chemistry of waters in Lake Qinghai catchments, NE Qinghai-Tibet plateau, China. *Quaternary International* 212, no. 1: 35–43.

Younas, A., N. Mushtaq, J.A. Khattak, T. Javed, H.U. Rehman, and A. Farooqi. 2019. High levels of fluoride contamination in groundwater of the semi-arid alluvial aquifers, Pakistan: Evaluating the recharge sources and geochemical identification via stable isotopes and other major elemental data. *Environmental Science and Pollution Research* 26, no. 35: 35728–35741.

Zhang, M.J., and S.J. Wang. 2016. A review of precipitation isotope studies in China: Basic pattern and hydrological process. *Journal of Geographical Sciences* 26, no. 7: 921–938.